DOI 10.5012/bkcs.2011.32.7.

Preparation of Porous $LaFeO_3$ Nanowires using AAO Template and Their Catalytic Properties

Kwang-Hyeon Ryu, Ji-Eun Im, Kang-Kyun Wang, Eil Heo,† Sung-Han Lee,†,* and Yong-Rok Kim*

*Department of Chemistry, Yonsei University, Seoul 120-749, Korea. *E-mail: yrkim@yonsei.ac.kr*
*†Department of Chemistry, Yonsei University, Wonju 220-710, Korea. *E-mail: shl2238@yonsei.ac.kr*
Received April 21, 2011, Accepted May 13, 2011

Key Words : $LaFeO_3$ perovskite catalyst, Porous nanowires, Oxidative coupling of methane

$LaBO_3$ (B=transition metal) perovskite oxides, which have well-defined structure and high thermal stability, have been widely studied on their physical and chemical properties. An interesting potential application of the perovskites as catalysts is their use for redox reactions.[1-5] $LaFeO_3$ perovskite oxide is one of highly active catalysts for oxidation of hydrocarbons and has been prepared by various synthetic methods including sol-gel method, sonochemical method, hydrothermal method, and polymerizable complex method.[6-9] However, since these methods start from solution precursors, they need calcining at relatively high temperatures to obtain the crystalline particles, which results in the formation of crystalline powder with small surface area.[10,11] The small surface area of $LaFeO_3$ powder may limit its potential use as catalyst.

Metal oxide catalyst is generally used in the form of fine powder to give a large surface area. Fine particles of metal oxide may agglomerate into large particles at high temperatures, which results in deactivation of the catalyst. Recently, ordered porous compounds having high surface areas such as MCM, SBA, and AAO have attracted much attention as new materials for support with high loading and dispersion of catalysts.[11-13] However, the nanostructures may be collapsed by a solid-state reaction between catalyst and support at high temperatures. Metal oxide in the form of porous nanowires or nanotubes may be an advantage for its application as non-supported catalyst owing to its high surface area. Anodic aluminum oxide (AAO) membranes have used as the templates for synthesizing one-dimensional structures in a previously inaccessible size range by inclusion chemistry. Because AAO membranes can be synthesized with controllable pore diameter in the range of 5-200 nm, they are favorably used as templates for preparing the metal oxides in the form of nanowire or nanotube. Until now, some ceramic nanowires and nanotubes have been successfully synthesized using AAO templates.[6,14-16]

In this work, porous $LaFeO_3$ perovskite nanowires were prepared using AAO template by a sol-gel method. Amphiphilic triblock copolymer (F127), which is widely used in the synthesis of nanostructured materials because its assemblies can lead to mesostructures, was employed to induce the formation of mesopores in the final oxide nanowires. The oxide nanowires were examined as catalysts for the oxidative coupling of methane in the temperature range of 650-800 °C at atmospheric pressure and their catalytic results were compared with the fine powder catalyst. The catalysts were characterized by XRD, FE-SEM, HR-TEM, and N_2 sorption measurements.

Experimental

Anodic aluminum oxide membrane with a dimension of 200 ± 20 nm pore size, 5 cm^2 area, and 60 μm thickness was obtained from Whatman Co. (Anodisc 13). Prior to use it as template, the membrane was immersed in a hot H_2O_2 (35.0%) solution for 30 min, subsequently treated in hot deionized water under agitation for 30 min, and dried at 90 °C. The resulting membrane was immersed in 10 wt % octadecylchlorosilane ($C_{18}H_{37}SiCl_3$, 90 + %, Aldrich-Sigma) solution dissolved in Ar-bubbled benzene (98%, Merck) under agitation for 12 h, where the membrane surface was modified from hydrophilic to hydrophobic. The hydrophobic membrane was recovered by the filtration, washed in benzene, and dried at 60 °C. Figure 1 shows FT-IR spectra of the AAO membrane before and after treatment with octadecylchlorosilane. The IR spectrum of the membrane after treatment with octadecylchlorosilane exhibits two absorption bands at 2850 cm^{-1} and 2927 cm^{-1}. The former is due to symmetric stretching of C-H in methyl group and the later is due to asymmetric stretching of C-H, suggesting that the membrane surface is hydrophobic.

$LaFeO_3$ nanowires were prepared from $La(NO_3)_3{\cdot}6H_2O$ (99.99%, Aldrich.) and $Fe(NO_3)_3{\cdot}9H_2O$ (99.999%, Aldrich). In a typical synthesis, 2.166 g $La(NO_3)_3{\cdot}6H_2O$ and 2.020 g $Fe(NO_3)_3{\cdot}9H_2O$ were dissolved into ethylene glycol (99.9%, Merck) under intense stirring. 1.0 g F127 triblock copolymer (BASF, average molecular weight; 12,600) was dissolved in ethanol (99.9%, Merck). Both the metal nitrate solution and the F127 solution were then mixed together under intense stirring for 2 h. The hydrophobic membrane was immersed in the precursor solution and agitated for 12 h. The precursor-inserted AAO membranes were maintained at 60 °C for 4 days, then heated up to 600 °C with a heating rate of 1 °C/min or 20 °C/min in air, held at 600 °C for 6 h, and subsequently cooled down to room temperature at a decreasing rate of 20 °C/min. The $LaFeO_3$ nanowires were

obtained by removing the template in 1 M NaOH solution at 60 °C for 12 h. The oxide nanowires were analyzed by X-ray powder diffraction (XRD) using a Philips X-pert MPD system equipped with Cu-Kα radiation (λ = 1.5418 Å). Field-emission scanning electron microscopy (FE-SEM) and high-resolution transmission electron microscopy (HR-TEM) analyses were performed for the oxide nanwires using a JSM 6700F and a JEOL 3010, respectively. N_2 sorption isotherms of the oxide nanowires were obtained at liquid nitrogen temperature using a Micrometrics automatic gas adsorption system (ASAP 2010). BET and BJH analyses were performed to determine the surface area and the pore size distribution, respectively.

The catalytic reaction was performed in a continuous flow reactor which consisted of quartz tube (0.8 cm i.d. and 3 cm length) sealed to 0.4-cm-i.d. quartz tubes on two ends. The feed flow rate of the reaction mixture at ambient condition was $CH_4/O_2/He=10/2/8$ cm^3/min and the purity of the gases was greater than 99.99%. The amount of catalyst used for this reaction was typically 15 mg. The gas products were analyzed by on-line gas chromatography equipped with a thermal conductivity detector (TCD) and a flame ionization detector (FID). Methane conversion and product selectivity were typically compared after 1 h time-on-stream.

Results and Discussion

In this work, the dissolution of lanthanum nitrate and iron nitrate in ethylene glycol formed glyoxylate anion: $C_2H_6O_2(l) + 2NO_3^-(aq) \rightarrow C_2H_2O_4^{2-}(aq) + 2NO(g) + 2H_2O$. During the calcination treatment of precursor-filled AAO membrane, solvents like ethanol and water were removed from the membrane, metal glyoxylates were decomposed into metal oxides by evolving $CO_2(g)$ and $H_2O(g)$, and $LaFeO_3$ oxide grew within the AAO pores to form the nanowires. Figure 2 shows typical FE-SEM images of the oxide before and after removing AAO template, indicating the oxide product in the form of nanowires. The length of the nanowires was less than 30 μm. Figure 3 exhibits the X-ray powder diffraction patterns of the oxide nanowires, indicating monophase $LaFeO_3$ perovskite oxide with orthorhombic structure. HR-TEM images of the oxide nanowires are shown in Figure 4, which reveals that many pores are irregularly distributed in the oxide nanowires. The pores may be interconnected to form channels in the oxide nanowires, but the channels were not clearly identified in this work. The pore size distributions obtained by the BJH analysis indicated the existence of mesopores in the oxide nanowires. Average pore sizes were 10.2 nm for the sample calcined with 1 °C/min and 6.4 nm for the sample calcined with 20 °C/min. BET surface areas were determined to be 28.5 m^2/g for the sample calcined with 1 °C/min and 21.7 m^2/g for the sample calcined with 20 °C/min.

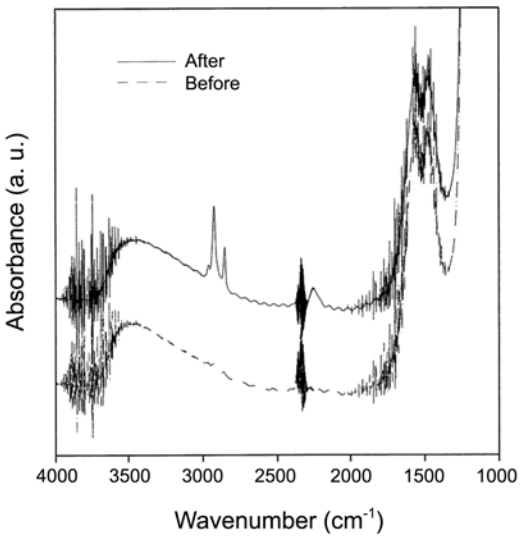

Figure 1. FT-IR spectra of AAO membrane before and after reaction with octadecylchlorosilane.

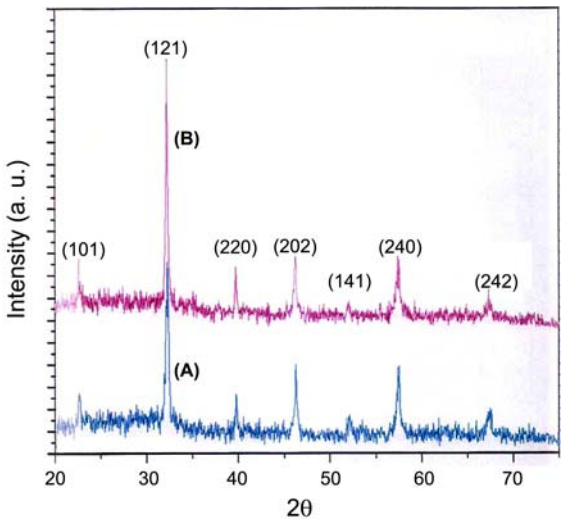

Figure 3. X-ray diffraction patterns of $LaFeO_3$ nanowires calcined with (A) 1 °C/min heating rate and (B) 20 °C/min heating rate during the calcination treatment. $LaFeO_3$ (JCPDS no. 37-1493).

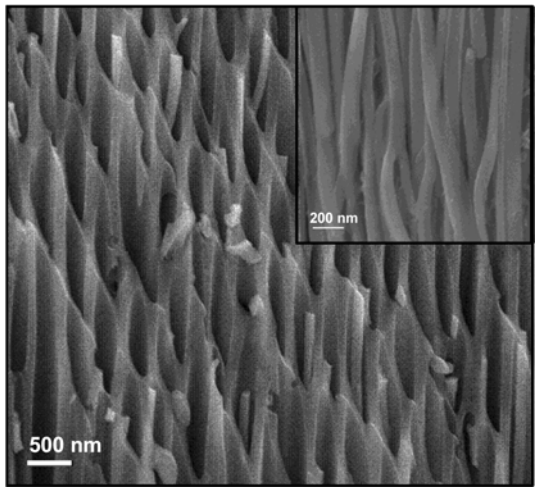

Figure 2. FE-SEM image of $LaFeO_3$ nanowires within AAO template calcined with 20 °C heating rate during the calcination treatment. The inset shows the oxide nanowires after removing the AAO template.

The oxide nanowires are considered to be composed of numerous cystal grains which are interconnected. We calculated average sizes of crystal grains, d, using the FWHM value of the (1 2 1) major peak, B, and Scherrer equation: $d=0.9\lambda/B\cos\theta$, where λ is the wavelength of the X-rays. The values calculated were 26.1 nm and 42.7 nm for the samples calcined with 1 °C/min and 20 °C/min, respectively. The result suggests that the crystal grain size (or the extended crystallinity) is controllable with heating rate during the calcination treatment. $LaFeO_3$ fine powder was prepared as a reference sample by the conventional citrate sol-gel method. The resultant $LaFeO_3$ fine powder, which was calcined at 600 °C with 20 °C/min heating rate, had a surface area of 5.3 m^2/g. Though the surface areas of the $LaFeO_3$ nanowires are lower than those of mesoporous materials like SBA15 and MCM41, their values are higher than that of the $LaFeO_3$ fine powder.

The $LaFeO_3$ oxides showed catalytic activities for the oxidative coupling of methane in the temperature range of 650-800 °C, in which CO_2, C_2H_4, and C_2H_6 were produced as major products and CO was scarcely produced. Figure 5 shows variations of CH_4 conversion and C_2 selectivity with temperature for the catalysts. At 800 °C, the $LaFeO_3$ nanowires calcined with 20 °C/min produced a C_2 yield of 13.9% with a C_2 selectivity of 57.7% and the fine powder produced a C_2 yield of 3.5% with a C_2 selectivity of 20.3%, which indicates that the nanowires are more active and selective than the fine powder in the reaction. The higher activity of nanowires is considered to be attributable to the higher surface area. As shown in Figure 5, the $LaFeO_3$ nanowires calcined with 20 °C/min showed higher activity than the nanowires calcined with 1 °C/min. Both samples calcined with 1 °C/min and 20 °C/min showed significant difference in the crystal grain size, but their surface areas didn't differ significantly, which enables us to consider that the extended crystallinity or the crystal grain size is directly related to the catalytic activity.

In general, the total oxidation of methane generally occurs below 500 °C while the oxidative coupling of methane takes place in the temperature range of 600-900 °C at high ratio of CH_4/O_2.[18] It is generally accepted for the oxidative coupling of methane that less electrophilic oxygen species like O^-(ads) and O_2^-(ads) on the surface of metal oxide catalyst act as active sites for methane.[18-20] The present catalysts produced C_2 hydrocarbons above 650 °C in the CH_4/O_2 reaction. Total activity of $LaFeO_3$ catalyst in the methane

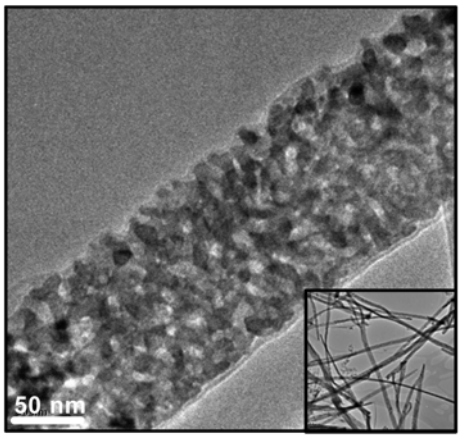

Figure 4. HR-TEM images of $LaFeO_3$ nanowires calcined with (a) 1 °C/min heating rate and (b) 20 °C/min heating rate during the calcination treatment.

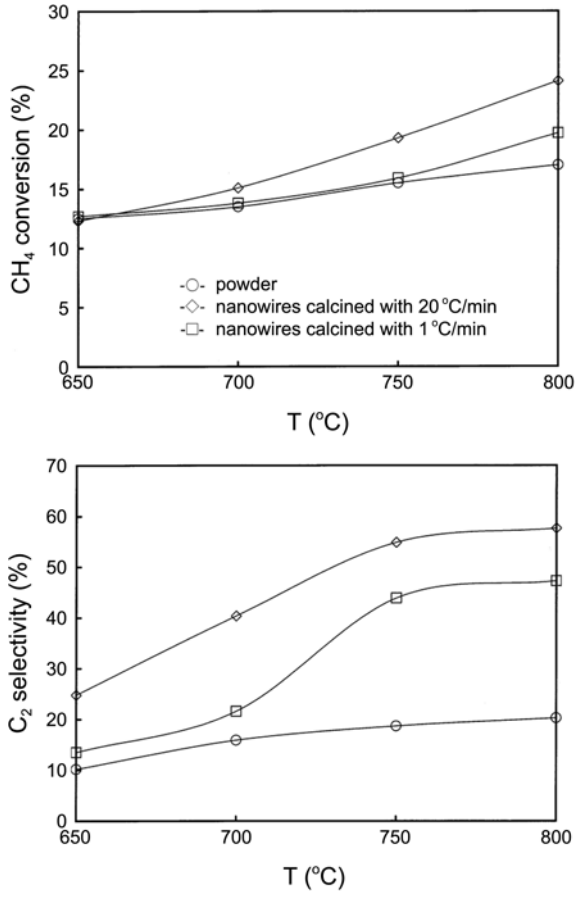

Figure 5. Variations of CH_4 conversion and C_2 selectivity with temperature for oxidative coupling of methane over $LaFeO_3$ fine powder prepared by citrate method (○) and porous $LaFeO_3$ nanowires calcined with 1 °C/min heating rate (□) and 20 °C/min heating rate (◇) during the calcination treatment.

oxidation has been explained by active oxygen species adsorbed on oxygen vacancies which are formed by the reduction of Fe^{3+} to Fe^{2+} in the oxide.[17] However, the origin of activity of $LaFeO_3$ catalyst for the oxidative coupling of methane may be different from the total oxidation because the oxidative coupling of methane occurs at higher temperatures. In case of $LaFeO_3$ perovskite, it has been proved that a small amounts of Fe^{3+} ions in the perovskite structure can be oxidized to Fe^{4+} ions during the calcination process at high temperatures.[21,22] The oxidation of Fe^{3+} to Fe^{4+} can induce a liberation of lanthanum ions from the perovskite lattice, based on the principle of controlled valency. The resulting lanthanum oxide should be related to the nature and reactivity of the perovskite surface. In the previous work,[23] we also reported the presence of the surface lanthanum oxide in the $LaFeO_3$ perovskite prepared by the citrate sol-gel method. Since lanthanum oxide catalyst is strongly basic and efficiently generate methyl radicals in the oxidative coupling of methane,[18] the catalytic activity of $LaFeO_3$ nanowires for the reaction is considered to be originated from the surface lanthanum oxide. In this work, the oxide nanowires with higher crystal grain size showed higher activity for the catalytic reaction, which implies that the surface lanthanum oxide is more rich in the oxide nanowires with higher crystal grain size.

In summary, the $LaFeO_3$ perovskite oxide nanowires were prepared from metal nitrates and amphiphilic tribolck copolymer (F127) using AAO membrane template by a sol-gel method. Compared to the $LaFeO_3$ fine powder prepared by the citrate method, the oxide nanowires showed higher surface area and much higher catalytic activity for the oxidative coupling of methane. The pore size distribution and the mean size of crystal grains in the $LaFeO_3$ nanowires varied with heating rate during the calcination treatment of the precursor-filled template. The extended crystallinity of $LaFeO_3$ nanowires seems to be closely related to the formation of surface lanthanum oxide which plays a major role as active phase in the oxidative coupling of methane.

Acknowledgments. This work was supported by the Korea Science and Engineering Foundation through the Pioneer Converging Technology Program (Grant No. 2010-0002190) and Basic Science Research Program (No. 2009-0077906).

References

1. Tejuca, L. G., Fierro, J. L. G., Eds.; *Properties and Applications of Perovskite-type Oxides*; Marcel Dekker Inc.: New York, 1993.
2. O'Connell, M.; Norman, A. K.; Huttermann, C. F.; Morris, M. A. *Catal. Today* **1999**, *47*, 123.
3. Spinicci, R.; Tofanari, A.; Faticanti, M.; Pettiti, I.; Porta, P. *J. Mole. Catal. A*: *Chemical* **2001**, *176*, 247.
4. Barbero, B. P.; Gamboa, J. A.; Cadus, L. E. *Appl. Cata. B*: *Environmental* **2006**, *65*, 21.
5. Spinicci, R.; Tofanari, A.; Delmastro, A.; Mazza, D.; Ronchetti, S. *Mat. Chem. Phys*. **2002**, *76*, 20.
6. Yang, Z.; Huang, Y.; Dong, B.; Li, H.-L. *Mat. Res. Bull.* **2006**, *41*, 274.
7. Sivakumar, M.; Gedanken, A.; Zhong, W.; Jiang, Y. H.; Du, Y. W.; Brukental, I.; Bhattacharya, D.; Yeshurun, Y.; Nowik, I. *J. Mat. Chem.* **2004**, *14*, 764.
8. Zheng, W. J.; Lin, R. H.; Peng, D. K.; Meng, G. Y. *Mater. Lett.* **2000**, *43*, 19.
9. Popa, M.; Frantti, J.; Kakihana, M. *Soild State Ionics* **2002**, *154*, 135.
10. Szabo, V.; Bassir, M.; Kaliaguine, Van Neste, S. *Appl. Catal. B*: *Environmetal* **2003**, *42*, 265.
11. Yi, N.; Cao, Y.; Su, Y.; Dai, W. L.; He, H. Y.; Fan, K. N. *J. Catal.* **2005**, *230*, 249.
12. Mizuno, M.; Fujii, H.; Igarashi, H.; Misono, M. *J. Am. Chem. Soc.* **1992**, *114*, 7151.
13. Jung, H.; Kim, J. W.; Cho, Y. G.; Jung, J. S.; Lee, S. H.; Choi, J. G. *Appl. Catal. A*: *General* **2009**, *368*, 50.
14. Zhixun, L.; Yan, F.; Xiaofang, Z.; Jiannian, Y. *Mat. Chem. Phys*. **2008**, *107*, 91.
15. Wang, F.; Huang, H.; Yang, S. *J. Eur. Cer. Soc.* **2009**, *29*, 1387.
16. Hu, Z.-A.; Wu, H.; Shang, X.; Lu, R.-J.; Li, H.-L. *Mat. Res. Bull.* **2006**, *41*, 1045.
17. O'Connell, M.; Norman, A. K.; Huttermann, C. F.; Morris, M. A. *Catalysis Today* **1999**, *47*, 123.
18. Lunsford, J. H. *Angew. Chem*. **1995**, *34*, 970.
19. Delmastro, A.; Mazza, D.; Ronchetti, S.; Vallino, M.; Spinicci, R.; Brovetto, P.; Salis, M. *Mat. Sci. Eng.* **2001**, *B79*, 140.
20. Lacombe, S.; Geanter, C.; Mirodatos, C. *J. Catal.* **1994**, *151*, 439.
21. Rida, K.; Benabbas, A.; Bouremmad, F.; Pena, M. A.; Sastre, E.; Martinez-Arias, A. *Appl. Catal. A*: *General* **2007**, *327*, 173.
22. Barbero, B.; Gamboa, J. A.; Cadus, L. E. *Appl. Catal. B* **2006**, *65*, 21.
23. Cho, Y.-G.; Choi, K.-H.; Kim, Y.-R.; Jung, J.-S.; Lee, S.-H. *Bull. Korean Chem. Soc*. **2009**, *30*, 1368.